iScience, Volume *28*

Supplemental information

DPANN symbiont of *Haloferax volcanii* accelerates xylan degradation by the non-host haloarchaeon *Halorhabdus* sp.

Oleg N. Reva, Violetta La Cono, Laura Marturano, Francesca Crisafi, Francesco Smedile, Manasi Mudaliyar, Debnath Ghosal, Elena A. Selivanova, Marina E. Ignatenko, Manuel Ferrer, Laura Fernandez-Lopez, Mart Krupovic, and Michail M. Yakimov

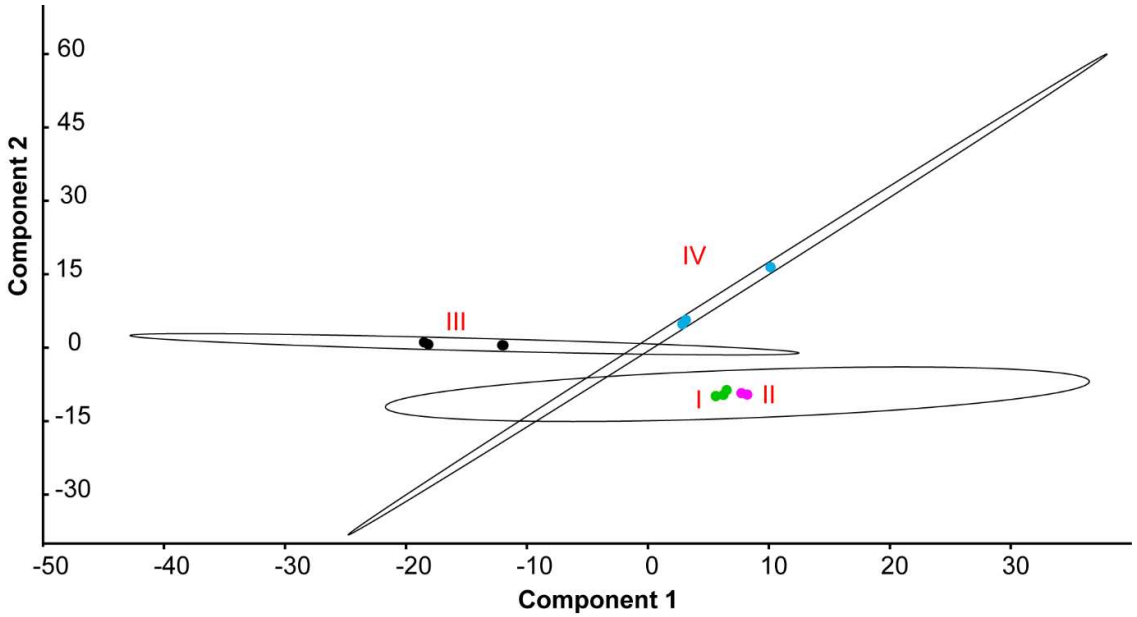

Suppl. Figure S1. The Principal Component Analysis (PCA) plot of the gene expression patterns of *H. volcanii* SVX82 in different consortia. Each repeated experiment is represented by nodes of consortium-specific colors and signed respectively: I) axenic monoculture on xylose; II) bipartite co-culture with *Ca.* N. occultus SVXNc on xylose; III) *Hr+Hv* bipartite culture; and IV) tripartite co-culture on xylan. Ellipses on the plot depict 95% confidence intervals estimated for different consortia.

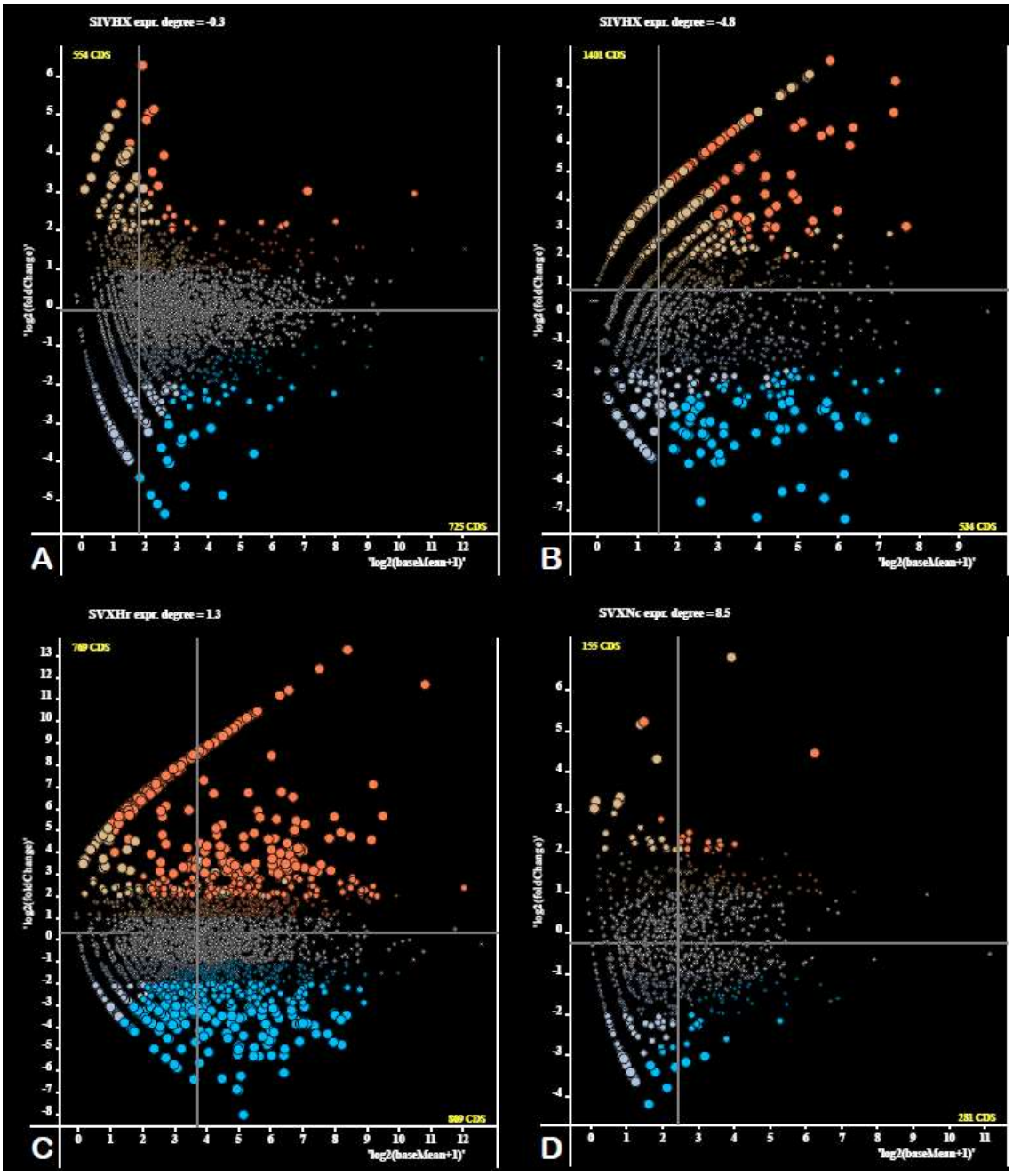

Suppl. Figure S2. M-Plots of gene regulation. Gene expression in A) *H. volcanii* SVX82 grown in the Hv+No bipartite culture with *Ca.* N. occultus SVXNc on xylose compared to its axenic culture grown on xylose; B) *H. volcanii* SVX82 grown in the tripartite culture with *Ca.* N. occultus SVXNc and *Halorhabdus* sp. SVX81 on xylan compared to the *Hr+Hv* bipartite culture with *Halorhabdus* sp. SVX81 grown on xylose; C) *Halorhabdus* sp. SVX81 grown in the tripartite culture with *H. volcanii* SVX82 and its ectosymbiont *Ca.* N. occultus SVXNc on xylan compared to the bipartite culture with *H. volcanii* SVX82 on xylan; D) DPANN

ectosymbiont *Ca.* N. occultus SVXNc grown in the tripartite culture with *H. volcanii* SVX82 and *Halorhabdus* sp. SVX81 on xylan compared to the *Hr+Hv* bipartite culture with *H. volcanii* SVX82 on xylose. Nodes depict individual genes up-regulated (yellow and red colors for $0.01 < p \leq 0.05$ and $p \leq 0.01$, respectively) or down-regulated (grey and blue colors for $0.01 < p \leq 0.05$ and $p \leq 0.01$, respectively) under the experimental condition compared to the control condition. Genes, which are not differentially expressed at these conditions ($Log_2(fold\_change) < 1$ and $p > 0.05$), are shown as small white nodes. The size of the nodes indicates the level of gene regulation: small nodes correspond to $Log_2(fold\_change) < 1$; middle-sized nodes correspond to $1 \leq Log_2(fold\_change) < 3$; and large nodes are used when $Log_2(fold\_change) \geq 3$.

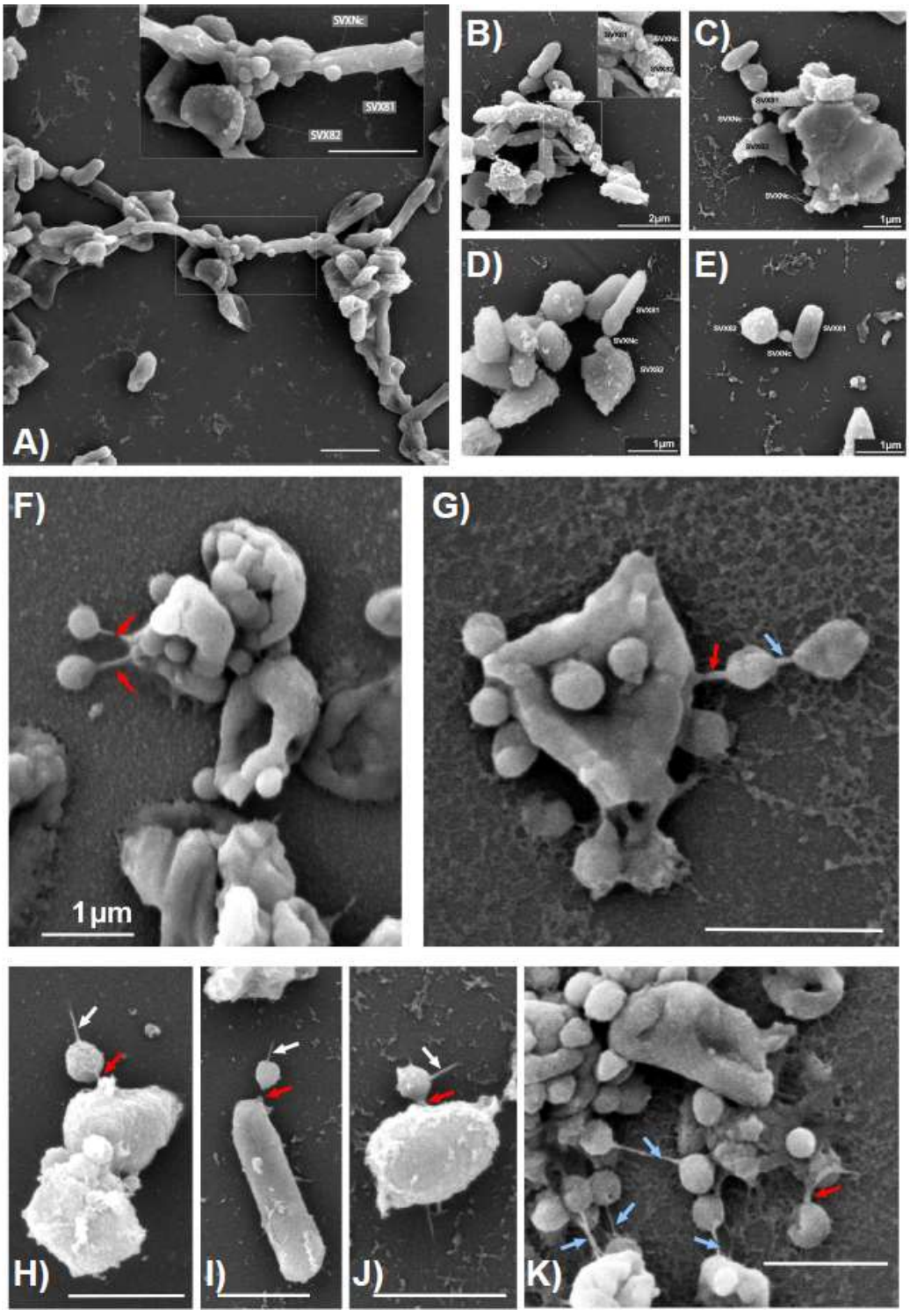

Suppl. Figure S3. Scanning electron microscopy (SEM) images of the heterocellular biofilm matrices created by cells of the tripartite xylan-degrading consortium grown on xylan. Scale bars correspond to 1 µm. A) Complex interactions between cells of *Halorhabdus* sp. SVX81, *H. volcanii* SVX82, and *Ca.* N. occultus SVXNc forming a

heterocellular biofilm; B-E) These snapshots demonstrate that several symbiotic cells are tightly attached at the same time to cells of two different hosts – *H. volcanii* SVX82 and *Halorhabdus* sp. SVX81; F-J) Thin and long protein stalks, as well as thick and short pilus-like structures or intracellular channels connecting either the ectosymbiont and host cells or the ectosymbiont cells themselves, are indicated by red and blue arrows, respectively. Long protein stalks resembling archaeal type IV pili systems are indicated by white arrows; K) Over-populated colonization of *H. volcanii* SVX82 cells by *Ca.* N. occultus SVXNc after one month of cultivating the tripartite culture on xylan.

Suppl. Table S2. Reads per Kilo base per Million mapped reads (RPKM) values of selected metabolic genes of *Haloferax volcanii* SVX82 characterized by significan difference in gene expression in the following archaeal consortia. I) Axenic monoculture on xylose; II) In a consortium with *Ca*. N. occultus SVXNc on xylose; III) With *Halorhabdus* sp. SVX81 on xylan; and IV) In a tripartite culture on xylan.

N	Gene*	Normalized RPKM values used for PCA				PCA coordinates		Product	Pathway
		I	II	III	IV	PC 1	PC 2		
1	SVXHx_2416	1.000	0.407	0.766	0.067	-0.065	-0.157	Multicopper oxidase	Mulitocopper oxidase
2	SVXHx_2424	0.704	0.168	1.000	0.064	-0.155	-0.090	Nitric oxide reductase large subunit	Nitric oxide reductase
3	SVXHx_2884	0.350	0.429	1.000	0.000	-0.167	-0.082	Phosphoserine phosphatase	L-serine biosynthesis I
4	SVXHx_2123	0.118	0.103	1.000	0.000	-0.206	-0.017	LPPG:FO 2-phospho-L-lactate transferase	factor 420 biosynthesis I (archaea)
5	SVXHx_2475	0.105	0.000	1.000	0.033	-0.211	0.003	NADPH:quinone reductase	NADPH:quinone reductase
6	SVXHx_0438	0.077	0.048	1.000	0.053	-0.208	0.007	Glyceraldehyde 3-phosphate dehydrogenase (phosphorylating)	gluconeogenesis I
7	SVXHx_0687	0.088	0.102	1.000	0.123	-0.198	0.016	Inorganic pyrophosphatase	Inorganic pyrophosphatase
8	SVXHx_0300	0.084	0.104	1.000	0.132	-0.197	0.018	Archaeal/vacuolar-type H+-ATPase subunit D	Archaeal/vacuolar-type H+-ATPase
9	SVXHx_2085	0.029	0.018	1.000	0.130	-0.207	0.034	2,3-bisphosphoglycerate-independent phosphoglycerate mutase	Entner-Doudoroff pathway III (semi-phosphorylative); gluconeogenesis I
10	SVXHx_1167	0.011	0.005	1.000	0.161	-0.207	0.045	ATPase involved in archaellum/pili biosynthesis	Archaellum pili biosynthesis
11	SVXHx_2192	0.056	0.064	1.000	0.238	-0.193	0.050	Translation elongation factor EF-1 alpha, GTPase	Translation elongation factor 1 alpha subunit
12	SVXHx_1116	0.069	0.017	1.000	0.266	-0.193	0.060	Glutaredoxin-dependent peroxiredoxin	Peroxiredoxin
13	SVXHx_0229	0.318	0.000	1.000	0.914	-0.124	0.176	Phosphoribosylpyrophosphate synthetase	PRPP biosynthesis
14	SVXHx_1814	0.295	0.207	1.000	0.256	0.071	0.200	Molybdenum cofactor biosynthesis protein A	molybdenum cofactor biosynthesis
15	SVXHx_2445	0.019	0.116	0.000	1.000	0.091	0.215	ABC-type transport system, periplasmic component	ABC-type dipeptide/oligopeptide/nickel transporter
16	SVXHx_2209	0.077	0.106	0.000	1.000	0.095	0.208	ABC-type Mn/Zn transport system, periplasmic component/surface adhesin	ABC-type Mn/Zn transporter
17	SVXHx_0081	0.160	0.059	0.000	1.000	0.098	0.202	Ammonium transporter	Ammonium transporter
18	SVXHx_1309	1.000	0.915	0.510	0.776	0.088	0.177	Fe-S cluster biogenesis protein NfuA, 4Fe-4S-binding domain	[2Fe-2S] iron-sulfur cluster biosynthesis
19	SVXHx_2186	0.585	1.000	0.000	0.219	0.100	0.187	Hydroxymethylglutaryl-CoA synthase	mevalonate pathway I (eukaryotes and bacteria); mevalonate pathway II (haloarchaea)
20	SVXHx_0075	0.291	0.188	0.000	1.000	0.116	0.170	Porphobilinogen deaminase	tetrapyrrole biosynthesis I (from glutamate)
21	SVXHx_2636	0.091	0.456	0.000	1.000	0.120	0.171	Isocitrate lyase	Glyoxylate shunt
22	SVXHx_1419	0.290	0.227	0.000	1.000	0.118	0.167	2-succinyl-5-enolpyruvyl-6-hydroxy-3-cyclohexene- 1-carboxylate synthase	Shikimate/chorismate biosynthesis (3-dehydroquinate synthesis in archaea)
23	SVXHx_2711	0.531	0.000	0.000	1.000	0.120	0.156	Phosphoribosyl 1,2-cyclic phosphate phosphodiesterase	Phosphoribosyl 1,2-cyclic phosphate phosphodiesterase
24	SVXHx_2868	0.437	0.227	0.000	1.000	0.128	0.146	Phenylalanyl-tRNA synthetase alpha subunit	tRNcharging
25	SVXHx_0624	0.250	0.681	0.013	1.000	0.143	0.126	Sulfide-dependent adenosine diphosphate thiazole synthase	Nicotinamide biosynthesis
26	SVXHx_2877	0.468	0.618	0.000	1.000	0.157	0.102	Pyruvate/2-oxoglutarate dehydrogenase complex, dehydrogenase (E1) component, alpha subunit	pyruvate decarboxylation to acetyl CoI
27	SVXHx_1310	0.533	0.634	0.000	1.000	0.163	0.092	Ribosome maturation protein Sdo1	Ribosome maturation
28	SVXHx_0532	0.538	0.974	0.000	1.000	0.187	0.057	tRNA(Ile)-lysidine synthase TilS/MesJ	tRNA(Ile)-lysidine synthase
29	SVXHx_0307	1.000	0.662	0.000	0.980	0.196	0.020	CTP-dependent Riboflavin kinase	Nicotinamide biosynthesis
30	SVXHx_1805	1.000	0.985	0.021	0.457	0.171	-0.133	ABC-type branched-chain amino acid transport system, periplasmic component	ABC-type branched-chain amino acid transporter
31	SVXHx_0440	0.838	1.000	0.000	0.000	0.127	-0.217	RimK family alpha-L-glutamate ligase	Alpha-L-Glutamate lyase
32	SVXHx_2751	1.000	0.816	0.000	0.000	0.126	-0.221	Uridylate kinase	Pyrimidine nucleobases salvage; UTP and CTP de novo biosynthesis
33	SVXHx_1400	1.000	0.810	0.000	0.000	0.126	-0.220	Mesaconyl-CoA hydratase (Acyl dehydratase family)	Mesaconyl-CoA hydratase
34	SVXHx_2300	1.000	0.600	0.000	0.000	0.112	-0.199	Siroheme synthase (precorrin-2 oxidase/ferrochelatase domain)	cob(II)yrinate a,c-diamide biosynthesis I (early cobalt insertion)
35	SVXHx_1734	1.000	0.516	0.000	0.000	0.106	-0.191	Na+/H+-dicarboxylate symporter	Na+/H+-dicarboxylate symporter
36	SVXHx_0561	1.000	0.500	0.000	0.000	0.105	-0.189	MBL fold metallo-hydrolase	Glutathione-dependent reactions
37	SVXHx_2460	1.000	0.500	0.000	0.000	0.105	-0.189	4-hydroxythreonine-4-phosphate dehydrogenase	4-hydroxythreonine-4-phosphate dehydrogenase
38	SVXHx_2468	1.000	0.348	0.024	0.021	0.091	-0.169	Galactitol PTS system EIIC component	Galactitol PTS system

*All genes exhibited two-fold or higher change in expression at least at one experimental setting, with a p-value of 0.05 or less